www.jpg.co.uk
Journal of Petroleum Geology

Journal of Petroleum Geology, Vol. 40(1), January 2017, pp 85 - 103

DEPOSITIONAL AND DIAGENETIC BARRIERS, BAFFLES AND CONDUITS: PERMIAN – CARBONIFEROUS UNAYZAH RESERVOIR, NUAYYIM FIELD, CENTRAL SAUDI ARABIA

K. Al-Ramadan[1*], S. G. Franks[2], S. Al-Shammari[3], A. Rees[3], A. Koeshidayatullah[1] and S. Abu-Khamsin[1]

The Unayzah Formation is one of the most important Palaeozoic reservoir systems in Saudi Arabia. In the Nuayyim field, Central Saudi Arabia, it produces light, sweet crude oil and consists of three main reservoir units, in descending stratigraphic order: Unayzah A, B and C. These reservoir units include a wide range of depositional facies deposited under a variety of climatic conditions, from high-latitude glacio-fluvial to more temperate playa/lacustrine, floodplain and braided-fluvial to hot-arid aeolian environments. Together with the diagenetic changes superimposed on the various depositional facies, this has produced complex reservoir heterogeneity.

The effects of this diagenetic and sedimentologic complexity on reservoir quality and compartmentalization are the subject of this paper. Approximately 816 ft of core and 611 core plug samples were examined from three wells which penetrate, completely or in part, the Unayzah reservoir. We combine petrographic and scanning electron microscope analysis with porosity and permeability data and calculated pore throat dimensions to identify fluid conduits, barriers and baffles to fluid flow. A rock classification scheme is proposed which takes into account whether the pore-level control on fluid flow is due to depositional or diagenetic processes and the composition of depositional or diagenetic phases within the pores. Distinguishing depositional versus diagenetic controls on fluid flow is important for predicting the three-dimensional geometry of conduits, barriers and baffles, and a priori knowledge of potential reactions between injected fluids and reservoir rocks is important for designing enhanced oil recovery fluids.

In the three wells studied, it appears that the Unayzah reservoir is compartmentalized vertically due to the occurrence of diagenetic and depositional barriers and baffles. There is insufficient data to assess the lateral or areal extent of the barriers, baffles and fluid conduits, but the understanding of pore-level controls on reservoir quality and the rock classification schemes introduced here will provide a starting point for future studies. These studies should combine well logs, seismic and engineering data with data presented here to assist mapping conduits, barriers and baffles across the field. The proposed classification schemes may also prove to be useful for assessing reservoirs in other fields both within Saudi Arabia and elsewhere.

[1] College of Petroleum Engineering and Geosciences, King Fahd University of Petroleum and Minerals, Dhahran, Saudi Arabia.
[2] RockFluid Systems, Inc., McKinney, TX, USA.
[3] Saudi Aramco, Dhahran, Saudi Arabia.
*author for correspondence, email: ramadank@kfupm.edu.sa

key words: Unayzah Formation, Saudi Arabia, diagenesis, reservoir quality, rock type, barriers, baffles, conduits, permeability, storage.

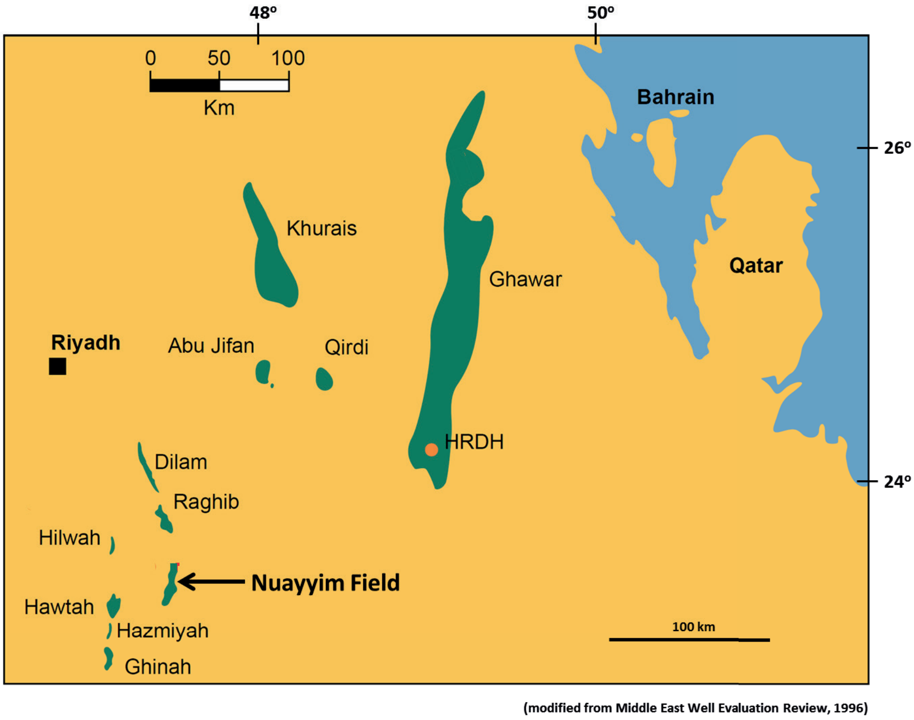

Fig. 1. Map showing the location of Nuayyim field in east central Saudi Arabia.

INTRODUCTION

The Unayzah Formation reservoir in Nuayyim field (Fig. 1) is a candidate for future enhanced oil recovery. The reservoir consists of sediments deposited under widely varying climatic conditions and depositional facies (Melvin and Sprague, 2006; Melvin *et al.*, 2010), and these significantly affect reservoir quality. The capacity for fluid storage and flow is affected by differences in grain size, texture and composition related to variations in depositional environments and climatic conditions. Diagenetic changes ranging from surface weathering to burial diagenesis also altered the three-dimensional pore-level structure of the reservoir. The extent to which these different factors affect fluid-flow properties and created barriers, baffles and conduits for fluid flow has not previously been determined or described. This study addresses these questions and provides a framework for future studies.

Ebanks *et al.* (1992) defined a "flow unit" as "*a mappable portion of the total reservoir within which geological and petrophysical properties that affect flow of fluids are consistent and predictably different from the properties of other reservoir rock volumes*." They emphasized the importance of identifying and mapping fluid flow units and listed the steps required:
(i) Identify the major lithofacies and vertical sequences from core and relate these to pore-level mineralogical and textural properties, porosity, permeability, capillarity and fluid saturations.
(ii) Determine the lithofacies which are responsible for fluid flow based on these pore-level properties.
(iii) Calibrate wireline logs to the major rock types, so that flow units may be correlated from well to well.
(iv) Establish the three-dimensional distribution of flow units using logs and a knowledge of the depositional environments.
(v) Test the validity of the model using production logs, flow tests, tracer surveys, water and hydrocarbon chemistry, and other similar types of data.

In this study we did not have access to well logs, fluid saturations or well tests and it was not therefore possible to carry out steps iii, iv and v. It should also be noted that the terms "storage" and "storage capacity" as used in this paper do not take into account water saturation; they refer only to porosity or porosity-feet (ϕh). However, we have: identified the primary pore-level controls on fluid flow; classified rock units as barriers, baffles and conduits; identified the primary mineral phases in pores which may potentially react with EOR fluids; and finally, have developed rock classifications which will assist in the planning for EOR projects and mapping flow units across Nuayyim field.

GEOLOGICAL BACKGROUND

The Unayzah Formation is the most prolific Permo-Carboniferous hydrocarbon reservoir in Central Saudi Arabia. It produces sulphur-free, light crude oil and sweet gas. The formation is divided informally into three reservoir units (Fig. 2), referred to as Unayzah A, B and C (McGillivray and Husseini, 1992), which collectively represent a wide range of depositional

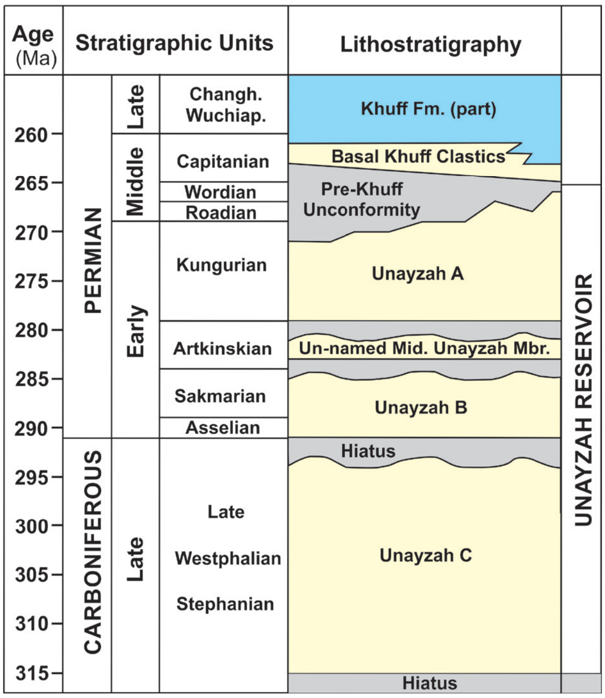

Fig. 2. Unayzah stratigraphic section (modified after Melvin and Sprague, 2006).

environments including alluvial fan, playa, braided fluvial, floodplain, aeolian dune and glacial outwash. Silurian source rocks beneath the "Hercynian" unconformity are the primary source of the oil and gas. Shales and paleosols in the overlying Permian-age Basal Khuff Clastics and shales and evaporites in the Khuff carbonates provide a vertical seal. The hydrocarbon geology of the Unayzah reservoir was discussed in detail by Konert *et al*. (2001), and readers are referred to this paper and references therein for a full description.

The stratigraphic and sedimentological characteristics of the Unayzah Formation have been extensively described in previous publications (Al-Laboun, 1987; McGillivray and Husseini, 1992; Aktas and Cocker, 1995; and Senalp and Al-Duaiji, 2001), and only a brief summary is given here. Deposition occurred during Late Carboniferous to Early Permian time when the Arabian Plate was moving from high southerly latitudes to more sub-tropical latitudes (Konert *et al*., 2001; Melvin *et al*, 2010).

The Unayzah C was deposited above the regional "Hercynian" unconformity during the mid-Carboniferous. The Unayzah C is composed of a thick sequence of clean, quartzose sandstones which are in general structureless to cryptically bedded, although low-angle cross-bedding, over-steepened beds, sand injection features and dewatering structures are locally observed. The sandstones are medium- to coarse-grained with stringers of granules and pebbles and greenish siltstones, and appear to have been rapidly deposited. Senalp and Duaji (2001) and Melvin and Sprague (2006) interpreted the Unayzah C as a glacio-fluvial outwash deposit associated with the retreat phase of the Late Palaeozoic Gondwanan glaciation.

Glacial streams of the Unayzah C gave way to meltwater-stage braided stream, lake and playa deposits of the Unayzah B as the Arabian Plate moved to lower latitudes. The Unayzah B sandstones, siltstones, shales and pebbly mudstones were deposited during glacial retreat (Senalp and Duaji, 2001; Melvin and Sprague, 2006). Sandstones are interpreted to have been deposited in braided streams and as sheet-flood deposits. Shales, silts, and some thin sands were deposited in glacial lakes and shallow playas. Pebbly mudstones, interpreted as glacial diamictites, are not represented in the three wells examined in this study but are known from the Unayzah in other wells.

During deposition of the Unayzah A, a hotter and more arid environment prevailed. The unit is composed of sandstones, conglomerates, red siltstones and mudstones deposited in a range of arid environments including braided ephemeral streams, playas, alluvial fans and aeolian dunes. Unayzah A time was punctuated by periods of higher humidity leading to periodic development of paleosols.

The Basal Khuff Clastics (BKC) succession rests unconformably on the Unayzah reservoir (Fig. 2) and consists of braided stream deposits, fluvial-estuarine sands and shales, and marginal marine sediments punctuated by thicker and more mature paleosols (Franks, 2008). These deposits were laid down under more humid climatic conditions. The Basal Khuff Clastics rest with significant erosional unconformity on the Unayzah reservoir, in some cases cutting out the upper Unayzah units. This so-called pre-Khuff unconformity (PKU) has been interpreted as a type II unconformity by Senalp and Duaji (2001), indicating a significant drop in sea level without a significant basinward shift of facies.

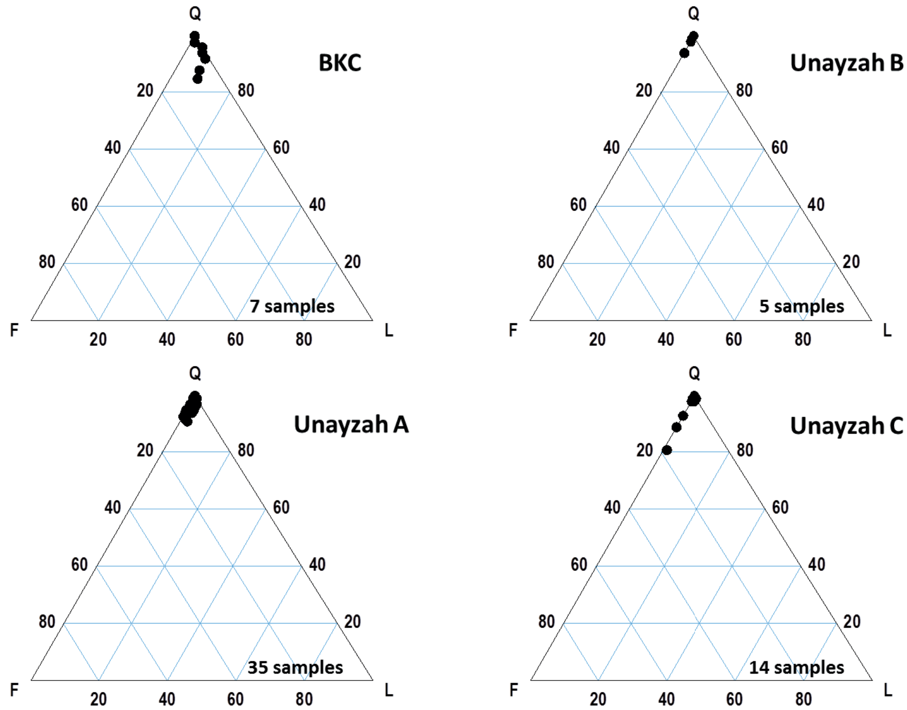

Fig. 3. QFL plots for all the Unayzah samples analysed. Basal Khuff Clastics (BKC) samples are quartz arenites to sublitharenites (Dott's 1964 classification). Unayzah A, B, and C samples are quartz arenites to subarkoses. Most Unayzah medium to coarse sandstones are quartz arenites. Very fine sandstones and siltstones are subarkosic.

MATERIALS AND METHODS

This study is based on core data from three wells in the Nuayyim field, referred to here as wells 1, 2 and 3. Core plugs and unstressed porosity/permeability measurements were provided by Saudi Aramco. More than 600 porosity/permeability measurements were made from the three cored wells. Plots of porosity versus permeability were made, and 61 samples were selected for thin section and SEM analysis based on the trends observed. The samples were point-counted for composition and visible porosity (using a 300-point count), and 100 counts for texture (grain size, sorting). X-ray diffraction (XRD) analyses (whole rock and clay) were also conducted on selected samples.

The porosity-permeability data were used to calculate permeability-feet (mD-feet or flow capacity, kh) and porosity-feet (storage capacity, ϕh) for different units and depositional facies and to construct modified stratigraphic Lorenz plots for the identification of barriers, baffles and conduits (c.f. Gunter *et al.*, 1997). Also, synthetic capillary pressure data were derived using published procedures (Pittman, 1992) to estimate the pore throat sizes of the different rock types. Porosity, permeability and pore throat dimensions were used in conjunction with petrographic data to establish a rock classification scheme of barriers, baffles and flow conduits which also takes into account the nature of the pore-filling or pore-lining phases and the origin of the phase, whether diagenetic or depositional.

The following sections present a general discussion of the petrographic data followed by the porosity and permeability data, and finally an integration of these data into two new rock classification systems.

RESULTS

Petrology of the Unayzah Reservoir

Sandstones of the Unayzah A, B and C are in general clean, very fine- to upper medium-grained, moderately well to well-sorted, sub-rounded to rounded quartz arenites to subarkoses (Fig. 3). Very fine sandstones to siltstones are more feldspar-rich than coarser-grained sandstones (Franks and Zwingmann, 2010). K-feldspar is more abundant than plagioclase (average K/P = 3.1). Lithic grains are predominantly fine-grained sedimentary rocks (mudstone, siltstone, fine sandstone).

Sandstones in the Basal Khuff Clastics are fine- to coarse-grained, moderately sorted, sub-rounded quartz arenites and sublitharenites. K-feldspar is considerably more abundant than plagioclase (average K/P = 14). Lithic grains are mostly fine-grained sedimentary rocks, including argillaceous and siliceous (chert) clasts of paleosols reworked from the upper Unayzah A and from within the Basal Khuff Clastics succession.

Diagenetic clays in the Unayzah and Basal Khuff Clastics include inherited and infiltrated/illuviated clay grain coats (cutans) (Fig. 4) as well as precipitated diagenetic clays (kaolinite, illite and chlorite). Clay

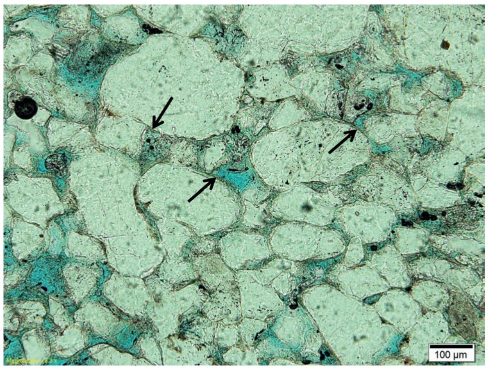

Fig. 4. Plane polarized light photomicrograph of an Unayzah A sandstone showing abundant clay-coated grains (arrows) and a low percentage of quartz overgrowths.

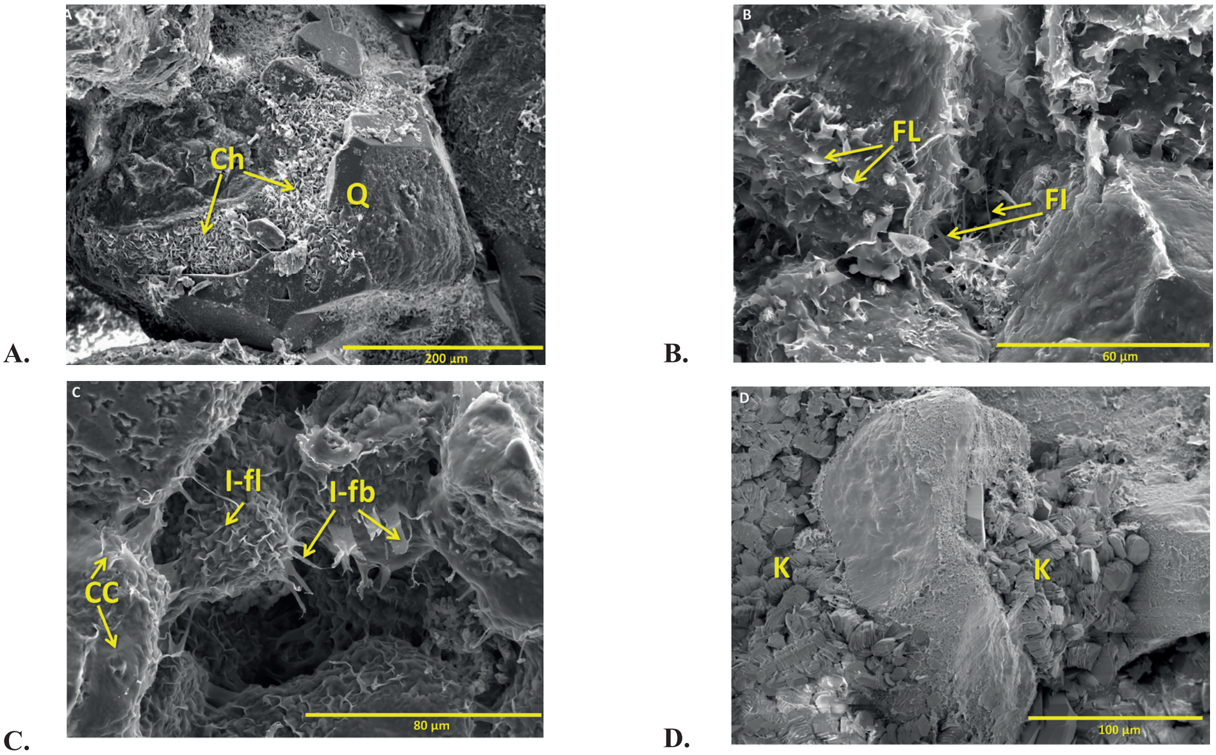

Fig. 5. SEM micrographs showing: (A) Grain-rimming chlorite platelets (Ch) partly engulfed by quartz overgrowths (Q); Unayzah C, braided fluvial sandstone, well 2 (250x). (B) Illite fibres (Fl) and flakes (FL) partly filling and bridging pores in Unayzah A aeolian dune sandstone; well 3. Flakes appear to grow from tangential clay coatings (cutans) and then to develop fibre-like projections from the margins (800 x). (C) Illite fibres (I-fb) and flakes (I-fl) partly filling and bridging pores in Unayzah A terminal fan sandstone, well 1. Flakes appear to grow from tangential clay coatings (CC) (cutans?) and then to develop fibre-like projections from the margins (750x). (D) Kaolinite booklets (K) plugging pores in Unayzah A braided fluvial sandstone, well 2 (450x).

cutans, in some cases exhibiting geopetal features, are more common in the Basal Khuff Clastics and Unayzah A than in the Unayzah B and C.

Precipitated pore-lining, pore-filling and grain-replacing clays are kaolinite, illite and chlorite (Table 1). Chlorite is most abundant in the Unayzah C, ranging from 0-5 %. It occurs primarily as grain-rimming platelets (Fig. 5a) but in some samples it fills pores or occurs as isolated rosettes within pores. It is rare in the Unayzah A and B and the overlying Basal Khuff Clastics.

Illite typically is present in the Unayzah A and B as well as the Basal Khuff Clastics but is less common in the Unayzah C. Illite most commonly occurs as irregular flakes which appear to grow from clay grain coats (cutans) (Fig. 5b). Illite fibres and ribbons appear to post-date the flakes. In some cases the fibres or ribbons appear to grow from the edges of the illite flakes (Fig. 5c).

Kaolinite is most abundant in the Basal Khuff Clastics sandstones which overlie the Unayzah reservoir. It is more common in the Unayzah A than in the Unayzah B and C (Table 1). Kaolinite replaces depositional matrix, replaces feldspar grains, and occurs as pore-filling cement (Fig. 5d).

Carbonate cements, mostly dolomite, are uncommon but are locally abundant in the Unayzah A and the Basal Khuff Clastics. Rarely, dolomite makes up 20-50 % of the rock volume. It is most common in paleosols (dolocretes) of the Unayzah A and the

Table 1. Distribution of diagenetic clays in the Basal Khuff Clastics (BKC) and Unayzah reservoir.

Stratigraphic unit	Kaolinite	Illite	Chlorite	Clay Cutans
BKC	11.5 (±6.6)	1.4 (±3.4)	0	1.1 (±2.0)
Unayzah A	2.8 (±2.5)	1.7 (±1.8)	0.3 (±1.0)	2.5 (±2.0)
Unayzah B	0.6 (±0.8)	1.5 (±2.2)	0	0.3 (±0.5)
Unayzah C	1.5 (±0.9)	0.4 (±1.2)	2.2 (±2.5)	0.1 (±.0.2)

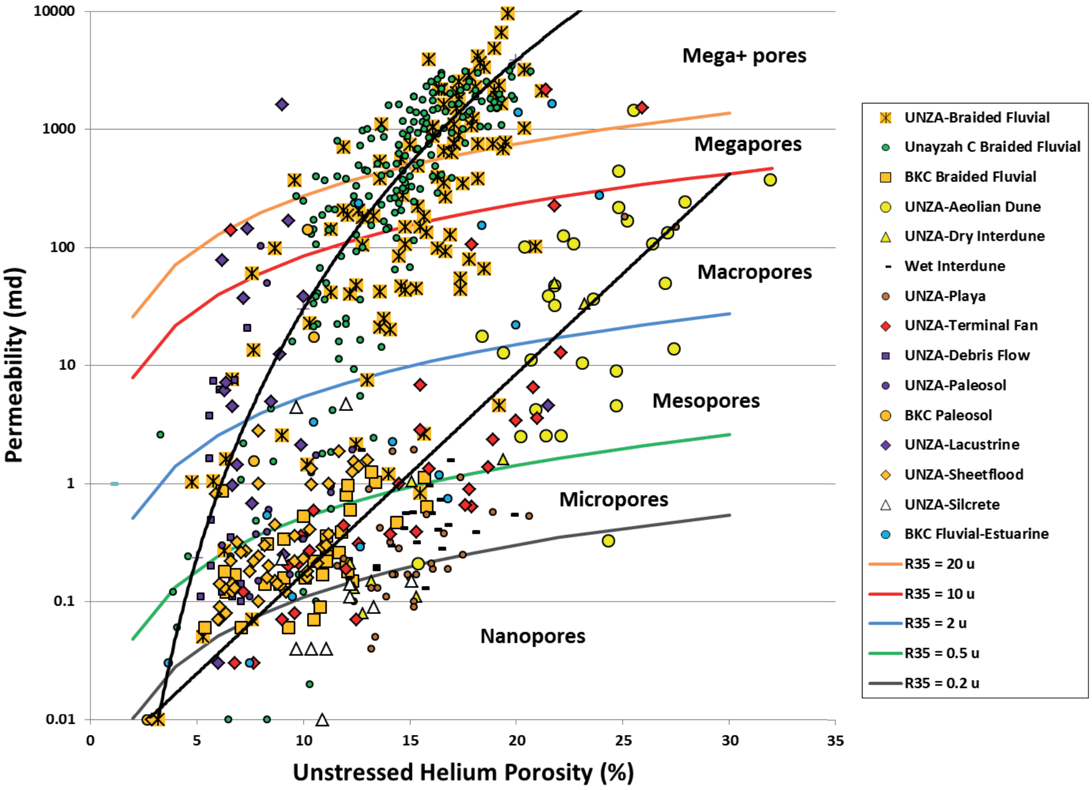

Fig. 6. Cross plot showing the relationship between porosity and permeability data from wells 1, 2, and 3 coded for depositional environment. The two black lines are not statistical fits but are "eye-ball" estimates of the poro-perm trends. The coloured lines are R_{35} pore throat radii calculated using the Winland equation (Kolodzie, 1980; Pittman, 2001).

Basal Khuff Clastics. Anhydrite also is found in some paleosols in proportions up to 20 %, in some cases accompanied by chalcedonic chert. The latter forms thick (5-10 ft) silcrete horizons in the upper Unayzah A in wells 1 and 3.

Haematite is present mostly in the Unayzah A, especially in the fine siltstones interpreted as playa and floodplain deposits. It also occurs as a grain coating in some Unayzah A sandstones. Total proportions are usually 1 % or less, but some aeolian and floodplain deposits of the Unayzah A have 2-6 % pore-lining and pore-filling haematite. It appears to contribute to microporosity in these samples.

Porosity and permeability

Porosity and permeability data for the three wells are shown in Fig. 6, identified by depositional environment. Two trends indicated by the solid black lines are evident, although each trend has considerable scatter. The upper trend is mostly defined by samples of Unayzah A and C braided fluvial sandstones from Wells 1 and 2. These samples have relatively high permeability for a given porosity. The trend is approximated by a power-law function (not a statistical best fit line):

Permeability (mD) = $3E\text{-}06(\phi_{He}{}^{7})$ (Eq. 1)

where ϕ_{He} is helium porosity in percent.

The lower trend is mostly represented by samples from wells 1 and 3 and includes most Basal Khuff Clastics braided stream sandstones, and Unayzah A aeolian-dune and sheetflood sandstones. It also includes Unayzah A wet interdune sandstones, playa siltstones and sandstones, and terminal fan sandstones. This lower trend demonstrates relatively low permeability for a given porosity. It can be approximated by an exponential function:

Permeability (mD) = $0.0035e^{0.39(\phi_{H\varepsilon})}$ (Eq. 2)

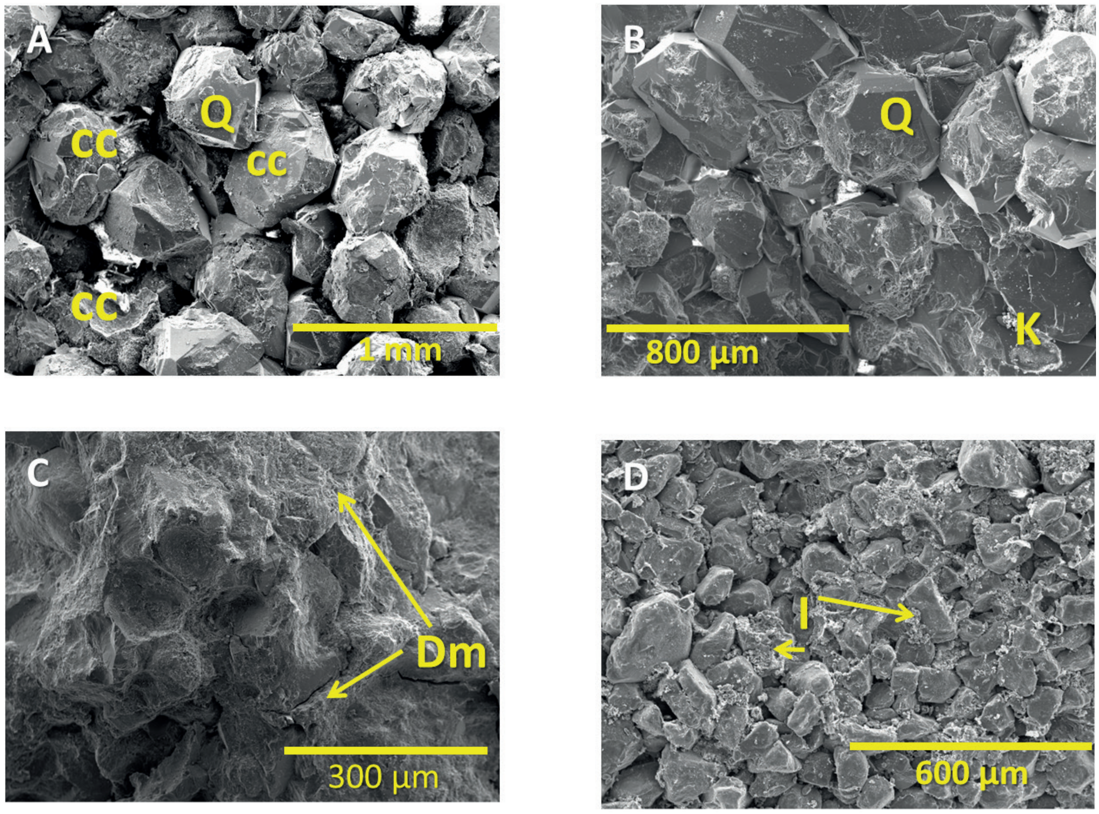

Fig. 7. SEM micrographs showing: (A) Unayzah A medium-grained braided fluvial sandstone, 19% porosity, k = 2126 mD; clay cutans (cc) have inhibited quartz overgrowths (Q) (50x). (B) Unayzah C medium-grained braided fluvial sandstone, 10.6% porosity, k =38.1 mD; quartz cement and minor kaolinite (K) have greatly reduced porosity and permeability (75x). (C) Basal Khuff Clastics medium-grained braided fluvial sandstone, 9.1% porosity, k = 0.34 mD; pores are plugged with densely-packed detrital clay matrix (Dm) (60x). (D) Unayzah A fine-grained aeolian dune sandstone, 24.3% porosity, k = 0.33 mD; flaky-to-fibrous illite (I) coats grains and plugs pores (100x).

Superimposed on Fig. 6 are R_{35} pore throat radii and pore throat classifications, from nanopores to mega+ pores, calculated using the so-called Winland equation (Kolodzie, 1980; Pittman, 2001):

$$\text{Log } R_{35} = 0.732 + 0.588 \log K_{air} - 0.864 \log \phi_{core} \quad \text{(Eq. 3)}$$

The R_{35} pore throat radii, representing the pore throat radii at 35% non-wetting phase saturation, is interpreted as the primary pore throat radius that controls fluid flow through the rock.

Unayzah A and C braided stream sandstones have large R_{35} pore throats, mostly greater than 10 microns (mega and mega+), and lie along the upper trend line in Fig. 6. These are in sharp contrast to braided stream sandstones of the Basal Khuff Clastics in which most R_{35} pore diameters are less than 0.5 microns (micro- and nanopores) and which lie at the lower end of the lower trend line in the figure. Only a few Unayzah A and C braided fluvial sandstones have such small pore throats.

Unayzah A aeolian dune sandstones also mostly lie along the lower porosity/permeability trend. They have 10 to 1000 times less permeability than braided stream sandstones of the Unayzah A and C with similar porosity. They have R_{35} pore throats mostly in the 0.5 to 10 micron range (meso- to macropores) but with some mega- and mega+ pores. Unayzah A wet interdune sandstones and Unayzah A playa siltstones and sandstones typically have micro- to nanopore throats. Unayzah A terminal fan sandstones lie along the lower trend and exhibit a good relationship between porosity and permeability. Their R_{35} values range from less than 0.2 microns to more than 20 microns.

Unayzah A lacustrine and debris flow samples together with many paleosols (e.g. Basal Khuff Clastics paleosols, Unayzah A silcretes) form a nearly vertical permeability trend, with porosity of 5 to 10 % and permeability ranging from less than 0.1 mD to more than 1000 mD (Fig. 6).

DISCUSSION

Both depositional (grain size and sorting) and diagenetic (cement and cement type) factors are responsible for the trends observed in Fig. 6. Coarser sandstones with little or no depositional matrix and low to moderate amounts of quartz overgrowth cement dominate samples at the high-porosity/high permeability end of the upper trend (Figs 6, 7a). These

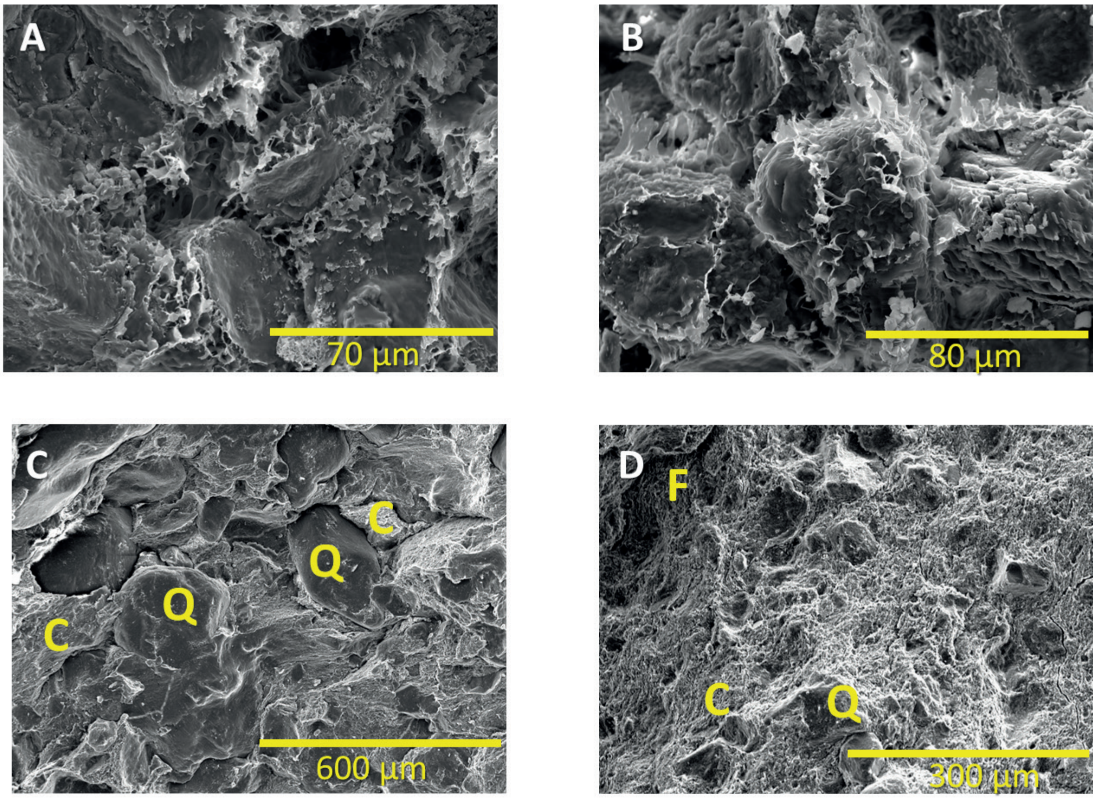

Fig. 8. SEM micrographs showing: (A) Unayzah A fine-grained terminal fan sandstone; fibrous to flaky illite coats grains and partly bridges pores; 22.1% porosity, k = 12.9 mD. (700x). (B) Unayzah A very fine-grained wet interdune sandstone; fibrous and flake-like illites line and bridge pore spaces; 16.8% porosity, k =1.58 mD (800x). (C) Unayzah A siliceous paleosol developed on braided stream sandstone; pores are plugged with clay (C), and microcrystalline quartz is present on some detrital quartz grains (Q); 12.3% porosity, k = 1.94 mD (100x). (D) Unayzah A argillaceous siltstone (playa/lacustrine), 9.3% porosity, k = 169 mD; silt and some fine quartz sand grains (Q) float in a clayey matrix (C). The reported high permeability is an artifact of sampling-induced microfractures (F).

are typically sandstones where clay cutans are present but are not thick enough to plug porosity, although they may inhibit quartz cementation. Quartz overgrowths are less well-developed in these sandstones, thus their porosity is higher. Sandstones with similar grain size and sorting but with less clay cutans are more cemented with quartz overgrowths, and their porosity and permeability are reduced (Fig. 7b). These sandstones plot along the low porosity/permeability part of the upper trend.

Basal Khuff Clastics braided stream sandstones have similar grain sizes to the Unayzah A, B and C braided stream sandstones, yet they fall at the low porosity – low permeability end (Fig. 7c) of the lower trend in Fig. 6. Abundant depositional clay matrix and pseudomatrix of compacted soil clasts has reduced both their original porosity and permeability. Unayzah A playa siltstones and very fine argillaceous sheetflood sandstones also plot in this part of Fig. 6.

Fine- to very fine-grained Unayzah A sandstones plot along the high porosity – high permeability end of the lower trend. Many of these are Unayzah A aeolian dune sandstones. Dune sandstones are fine grained, and pore throats and pores are partly plugged with diagenetic illite and kaolinite (Fig. 7d). Much of the reported helium porosity is microporosity within diagenetic clay and is ineffective for fluid flow. Some dune sandstones have permeability of hundreds of millidarcies. The differences in grain size and diagenetic clay along the trend are very subtle, yet they seem to make a significant difference in permeability.

Unayzah A terminal fan and wet interdune sandstones also plot along the lower porosity/permeability trend. Both are fine to very fine-grained with relatively low permeability for their reported porosity (Fig. 6). Flaky to fibrous diagenetic illite lines and partly bridges pores in these sandstones, greatly reducing their permeability (Fig. 8a, b). Abundant microporosity in the diagenetic illite accounts for the reported high helium porosity. The diagenetic illite appears in some cases to be forming by recrystallization of early infiltrated/illuviated clay coats, but Franks and Zwingman (2010) have shown that diagenetic illite in the Unayzah also forms from the reaction of kaolinite and K-feldspar during burial diagenesis. As with the dune sandstones, seemingly insignificant differences in texture, grain size and diagenetic clay content may result in order-of-magnitude differences in

Table 2. Microporous phases in Unayzah and Basal Khuff Clastics samples. Fractional microporosity for illite is the average reported by Sardini *et al.* (2009). Chlorite and kaolinite are the average values reported by Hurst and Nadeau (1995). Microporosity of the other phases was determined by trial and error to get the fit shown in Fig. 9b.

Phase	Illite	Chlorite	Kaolinite	Depositional Matrix	Pseudo-matrix	Cutans	Clay Laminae	Haematite
Fractional Micro-porosity	0.7	0.5	0.43	0.15	0.1	0.7	0.15	0.3

permeability with relatively small changes in porosity, as illustrated in Fig. 8a and 8b.

Unayzah A lacustrine, debris flow and paleosol samples with relatively low porosity (5-8%) exhibit a very wide range of permeability, from hundreds to more than 1000 mD, forming a nearly vertical trend in Fig. 6. SEM examination and petrographic analysis of these samples show no visible intergranular porosity (Fig. 8c,d). The low helium porosity is mostly ineffective microporosity within the clay matrix. The high permeability reported for some of these samples appears to be due to microfractures, which are observed in thin section and some SEM images. There is no mineralization or other evidence to suggest that these are natural fractures, and examination of the slabbed core from which the plugs revealed no microfractures. It appears, therefore, that the microfractures were induced either during plugging operations or subsequent handling in the laboratory. Comparison of these samples with similar samples without microfractures suggests that their permeability is most likely less than 1 mD, perhaps lower.

Effective porosity versus microporosity

Helium porosity reported for many samples significantly exceeds visible, thin-section porosity. Samples with no visible porosity have reported helium porosity of 4-12 % and there is a very poor relationship between helium porosity and thin-section porosity (Fig. 9a). This difference between helium porosity and thin-section porosity is sometimes unofficially referred to as "microporosity" by petrographers, without specifying how the microporosity is distributed among microporous phases. However, there have been previous attempts to quantitatively determine the amounts of microporosity present in different diagenetic clays. Hurst and Nadeau (1999), using image analysis on back-scattered SEM photos of various diagenetic clays, reported an average microporosity in kaolinite of 43 % with a range of 15-61 %. They reported average illite microporosity as 64 % with a range of 47-76 %. For chlorite platelets, Hurst and Nadeau (1999) reported that the microporosity range is 44-58 % with an average of 51 %. Sardini *et al*. (2009) found similar values for kaolinite (42%) but somewhat higher average illite microporosity (70%) using samples impregnated with a radioactive tracer.

Microporous phases identified petrographically in the Unayzah reservoir and the Basal Khuff Clastics are listed in Table 2. Using average values of microporosity reported previously for illite, kaolinite and chlorite, a good fit between helium porosity and point-counted thin section porosity can be obtained when microporosity values for depositional matrix, pseudomatrix, clay cutans, and clay laminae are assumed. The fit was slightly improved (R^2 from 0.71 to 0.73) by assigning microporosity to grain-coating and pore-filling haematite (Table 2; Fig. 9b).

Barriers, baffles and conduits

In this section, rocks of the Unayzah reservoir and the overlying Basal Khuff Clastics are described as flow conduits, barrier or baffles and their pore-level character is discussed. We propose and describe rock classification schemes which can be applied to assist with future EOR projects and show how these relate to the depositional and diagenetic character of the rock and the stratigraphy of the reservoir.

Rock type classification

Archie (1950) used the term "rock type" to refer to rocks with similar pore size distribution, porosity, permeability, capillary pressure and connate water saturation. In the absence of water saturation data and measured capillary pressures, perhaps the most straightforward way of typing Unayzah reservoir rocks and classifying them in terms of barriers, baffles and conduits is to consider their porosity and permeability and the calculated R_{35} pore throat radii. Considering the data shown in Fig. 6 and the preceding discussion of the effects of grain size, diagenetic phases, depositional matrix and other pore-filling and pore-lining phases, there appear to be natural sub-divisions which can be used to divide the Unayzah and Basal Khuff Clastics in the Nuayyim field into six rock types (Table 3).

Type I rocks are the best reservoir rocks with high porosity and permeability, and large pore throat radii. They have both high storage and high flow capacity. These are mostly medium to coarse sandstones deposited in braided fluvial systems in the Unayzah A, B and C. They are partly cemented with quartz overgrowths and may contain small amounts of diagenetic kaolinite (Fig. 10a). They are generally clean sandstones with less than 5% depositional matrix.

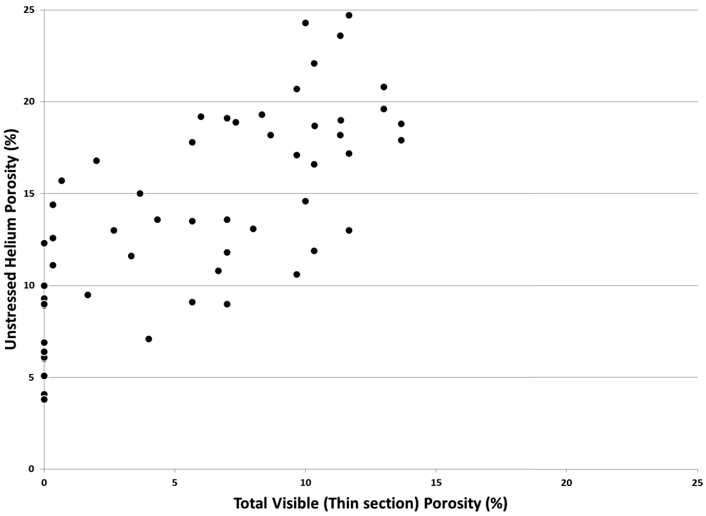

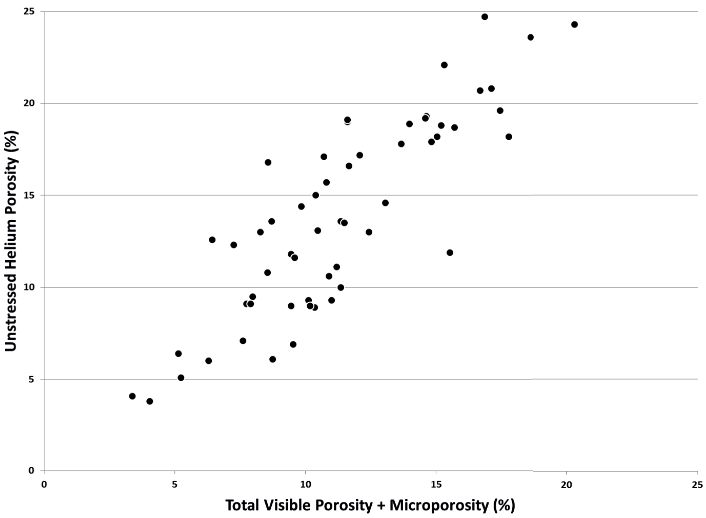

Fig. 9. Cross plots showing: (A, above). Total visible or point-counted thin-section porosity versus helium porosity on the same core plugs. (B, below). Total visible or point-counted thin-section porosity + microporosity versus helium porosity. Microporosity fraction of different clays was used to maximize the correlation. Values of microporosity for each phase are given in Table 2. $R^2 = 0.73$; $y = 1.2x + 0.24$.

Type II rocks are those with more than 10% porosity and permeability of 10-100 mD. Pore throat radii are in the 2-10 micron range (macropores). Coarser type II rocks are usually partly cemented with quartz overgrowths, similar to type I but with more cement. These are mostly Unayzah A and C braided stream sandstones. Finer-grained type II rocks are mostly Unayzah A dune, dry interdune, and terminal fan sandstones (Fig. 10b). The primary cements are kaolinite and illite. Thin clay cutans are commonly present. Overall type II rocks have good storage and flow capacity (Table 3).

Rocks in type III comprise those with porosity greater than 10 % and permeability of 1-10 mD. Pore throat radii are about 0.5 to 2 microns (mesopores). This rock type includes some fine- to medium-grained Unayzah A braided fluvial sandstones with moderate quartz cement and diagenetic illite as well fine- to very fine-grained aeolian dune and terminal fan sandstones with up to 10% diagenetic illite+kaolinite. These are low-flow conduits (Fig. 10c).

Rock type IV samples have moderate to high porosity and low permeability (>10%, <1 mD) and are dominated by diagenetic clay or a combination of diagenetic and depositional clay matrix. Pore throat radii are mostly in the micropore size (0.5-0.2 microns) with some <0.2 microns (nanopores). The rocks are mostly siltstone to very fine sandstone, although a few fine- to medium-grained sandstones with high amounts of depositional matrix are included in this category. While potentially they contribute to storage, their flow capacity is limited. This rock type is expected to be a barrier to fluid flow.

Type V rocks are those with both low porosity and low permeability (<10%, <1 mD). They are dominated mostly by pore-filling detrital clay and pseudomatrix. These pore-filling phases have relatively low microporosity compared to diagenetic clays (Table 2), and therefore they have low storage capacity and as well as low flow capacity. Pore throat radii are mostly classified as micro- and nanopores (<0.5 and <0.2 microns, respectively, Fig. 6). For all effective purposes, these may be considered strong barriers to fluid flow. Samples that fall into this category have a wide range of grain sizes from silt to upper medium sand.

Table 3. Rock type classification and description. See SEM micrographs in Fig. 10.

Rock Type	I (Flow conduit: High storage and flow capacity)	II (Flow conduit: Good storage and flow capacity)	III (Baffle:Fair storage and flow capacity)	IV (Barrier: Fair storage, low flow capacity)	V (Barrier: Low storage and low flow capacity)	VI (Fractured Barriers & High Flow, Low storage)
Helium Porosity %	>10	>10	>10	>10	<10	<10
Permeability mD	100-10000	10-100	1-10	<1.0	<1.0	1-1000
R35 microns	>10	10-2	0.5-2	<0.5	<0.5	0.5 - 20
Pore Class	Mega, Mega+	Macro	Meso	Micro, Nano	Micro, Nano	Meso,Mega, Mega+
Grain size (mm)	0.25 to > 0.50	0.09 – 0.35	0.09-0.13	0.25-0.35 (BKC) 0.02-0.09 (Unayzah A)	0.25-0.35 (BKC) 0.06-0.35 (Unayzah A)	0.02 – 0.35
Common Phases in Pores	Quartz overgrowths > chlorite, kaolinite, cutans	Quartz overgrowths; Cutans, kaolinite, chlorite, illite	Kaolinite > illite, cutans, depositional clay	Depositional clay matrix (BKC); illite, kaolinite, cutans (A)	Depositional and illuviated clay, cutans, illite	Depositional clay or quartz overgrowths
Key Unit/Environment	Unayzah A and C Braided Fluvial	Unayzah A and C braided fluvial, Unayzah A aeolian dunes	Unayzah A braided stream, aeolian dune, terminal fan, sheetflood	Unayzah A wet and dry interdune, terminal fan, sheetflood; BKC braided fluvial	Unayzah A sheetflood, paleosols; BKC braided fluvial	Unayzah A paleosols, lacustrine, debris flows, some braided fluvial
SEM micrograph	Figure 10a	Figure 10b	Figure 10c	Figure 10d	Figure 10e	Figure 10f

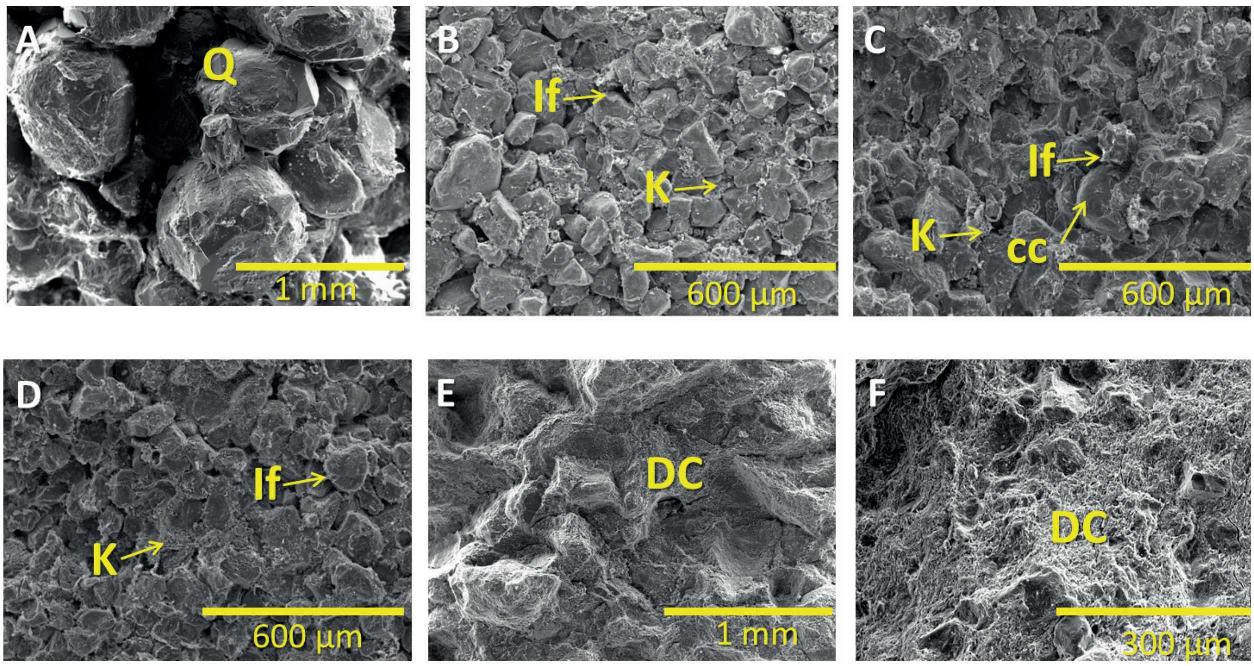

Fig. 10. SEM micrographs showing the rock types: (A) Type I (19.3%, 6610 mD), Unayzah A braided fluvial, coarse grained, partly quartz cemented (Q) sandstone (50x). (B) Type II (20.7%, 11.12 mD), Unayzah A aeolian dune sandstone with clay cutans, fibrous illite (If) and kaolinite (K) (100x). (C) Type III (19.2%, 4.57 mD), Unayzah A braided fluvial sandstone with clay cutans (cc), kaolinite (K) and fibrous-to-flaky illite (If) (100x). (D) Type IV (17.8%, 0.89 mD), Unayzah A terminal fan sandstone, with extensive fibrous illite (If) and kaolinite (K) (100x). (E) Type V (9.3%, 0.06 mD), Basal Khuff Clastics braided fluvial, medium grained sansdstone, mostly plugged with depositional clay matrix (DC) (50x). (F) Type VI (9.3%, 168.92 mD), Unayzah A playa/lacustrine, argillaceous siltstone, pores plugged with depositional clay (DC) (200x).

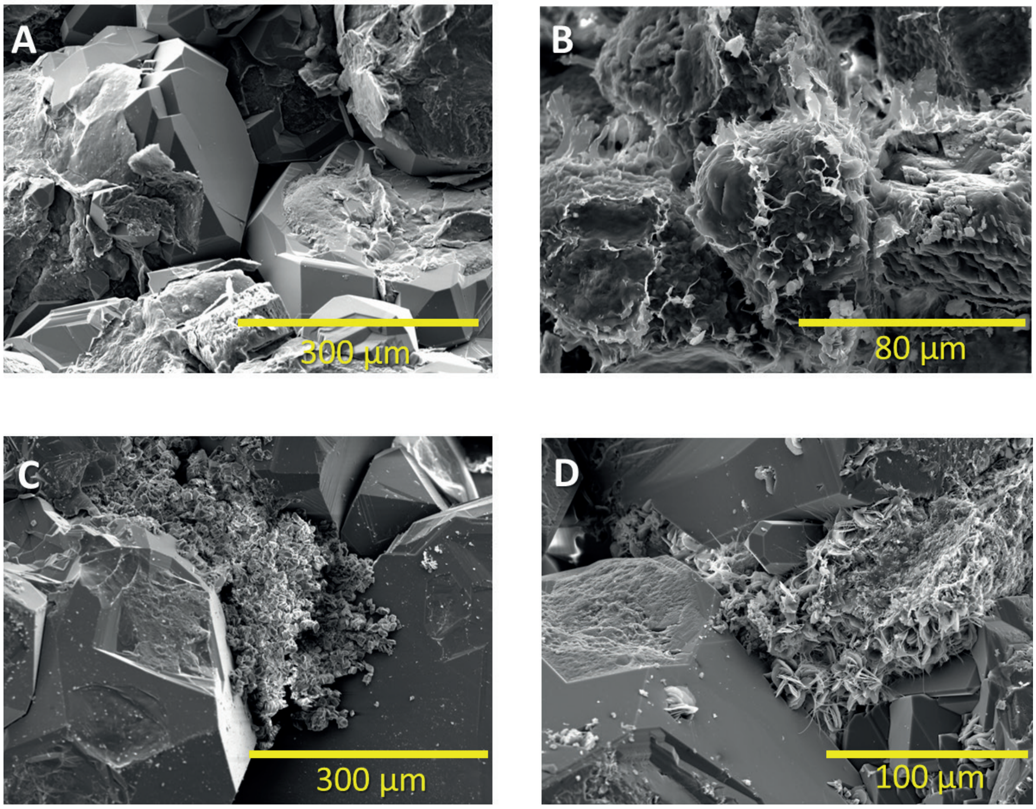

Fig. 11. SEM micrographs showing: (A) Unayzah A braided fluvial sandstone, rock type II (13.6%, 20.94 mD) 200x. (B) Unayzah A terminal fan sandstone, rock type II (22.1%, 12.9 mD) 700x. (C) Unayzah C braided stream sandstone, rock type II (10.8%, 66.71 mD) 200x. (D) Unayzah C braided fluvial sandstone, rock type II (11.8%, 83.45 mD) 500x.

Some core plugs consisting of siltstone and very fine argillaceous sandstone (e.g. playa/lacustrine and debris flows) have porosity less than 10 % but exhibit a very wide range of permeability (1 to >1000 mD). Calculated R_{35} pore throat radii range from 0.5 (mesopores) to more than 20 microns (mega and mega+ pores). Petrographic and SEM examination shows that most of the higher permeability samples have no visible porosity which could account for the reported permeability. Some contain visible microfractures which, it has been argued previously, are likely to be an artefact of sampling. Therefore, many of these samples should properly be classified as type VI.

However, there are several Unayzah A braided fluvial sandstones that have quite high permeability (10-100s mD) and low porosity (<10%). Their relatively low-porosity, high-permeability character is due to relatively coarse grain size, a lack of significant diagenetic or depositional clay, and partial cementation by quartz overgrowths. The large, slot-like pores between quartz overgrowths are clean and well connected, apparently accounting for the relatively high permeability.

The six-fold rock classification (Table 3) is useful for considering and mapping fluid storage and flow capacity. However, there are other, pore-level attributes which also are important considerations, such as the potential reactivity of the rock with injected fluids or potential for migrating fines. These relate to the nature of pore-filling and pore-lining cements, for example the shapes of the phases, their arrangement within pores and their composition. Archie (1950) anticipated such classifications and stated that: "…*the mineral composition of the rock should not be neglected in a study of these relationships. It must be recognized that the type of clay minerals present, for example, will no doubt play a greater role in the future*."

Mineralogy and composition are not accounted for in a classification based solely on porosity, permeability or capillarity (pore throat dimensions), except indirectly by how they affect capillarity. For example, samples which are classified as the same rock type using porosity, permeability, and pore throat radii may lie along either the upper trend of Fig. 6 (equation 1) or along the lower trend (equation 2). These differences, as previously noted, are due not only to grain size but to factors such as the importance of depositional versus diagenetic clay or type of diagenetic clay, as noted in Table 3.

An example of this is the upper medium-grained Unayzah A braided stream sandstones classified as type II by porosity, permeability, and R_{35} pore throat radii. These type II sandstones have pores formed by the clean, crystal faces of quartz overgrowths (Fig. 11a), whereas a type II Unayzah A terminal fan sandstone has pores lined and partly bridged by flaky/fibrous

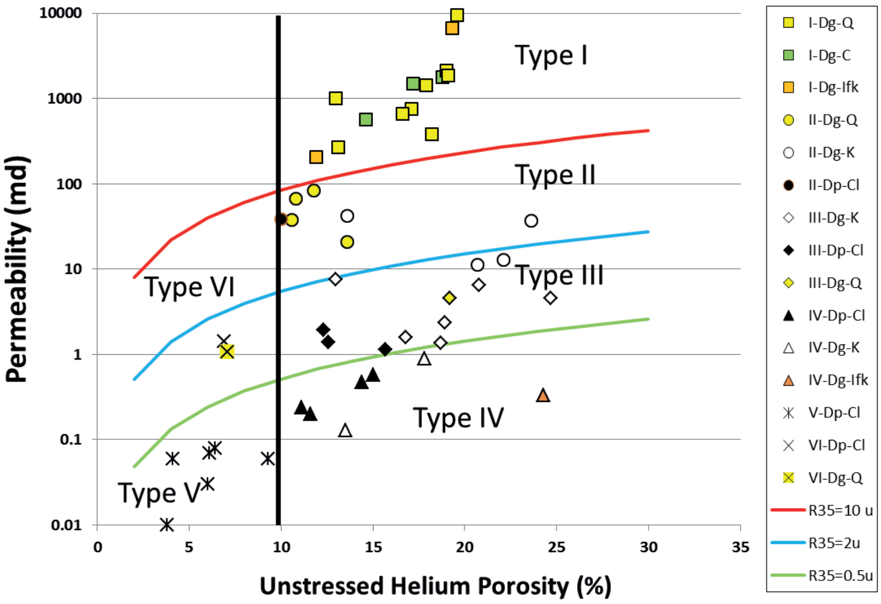

Fig. 12. Samples classified by porosity, permeability and R_{35} pore throat radius, together with the nature of the dominant pore-filling phase. Dg = diagenetic, Dp = depositional. Q = quartz overgrowths, C = chlorite, Ifk = flaky illite, Ifb = fibrous illite, and Cl = clay matrix undifferentiated. Samples with induced fractures have not been plotted.

illite (Fig. 11b). Likewise, type II Unayzah C braided stream sandstones have pores that are in some cases partly plugged by fine booklets of kaolinite (Fig. 11c) and in others are partly plugged with rosettes of chlorite (Fig. 11d). The potential for chemical reactivity or fines migration in each of these type II sandstones will be quite different (e.g. see the review by Wilson *et al*., 2014).

Taking these factors into account, the six-fold rock type classification (I-VI) has been modified. In addition to assigning a sample to one of the six rock types, the origin of the pore-lining or pore-filling phase is described as dominantly diagenetic (Dg) or depositional (Dp). Next, the composition of the phase which would be in contact with pore fluids is indicated such as kaolinite (K), illite (fibrous, Ifb; flaky, Ifl), chlorite (C), quartz (Q). Abbreviations for other diagenetic phases (e.g. D for dolomite) may be developed as needed. In the case of depositional matrix when the composition may not be certain, for example from petrographic observation alone, it can be denoted simply as depositional clay (Dp-Cl). For example, type IV-Dp-Cl is a barrier formed by depositional clay. Type I-Dg-Q is a flow conduit with diagenetic quartz overgrowths forming the pore walls, and II-Dg-Ifb is a flow conduit in which diagenetic fibrous illite dominates the pores.

Petrographic data are not available for all 611 samples; however, when the petrographic samples are classified in this manner, the best flow conduits, Type I, are mostly Type I-Dg-Q and I-Dg-C (Fig. 12). Type I-Dg-Q will be the least chemically reactive flow conduits. Type I-Dg-C are susceptible to reactions with acidic fluids, as both Fe-rich and Mg-rich chlorite may react (Wilson *et al*., 2014).

Type II flow conduits are mostly II-Dg-Q and II-Dg-K. These are chemically stable as neither quartz nor kaolinite are likely to react with injected fluids. However, kaolinite may be dislodged and migrate into pore throats, physically blocking them as originally suggested by Gray and Rex (1966). Wilson *et al.* (2014) discussed the migration of kaolinite in reservoir rocks and reviewed the effects of pH on kaolinite dispersion.

Type III baffles are mostly III-Dg-K, III-Dg-Ifk,Ifb, and III-Dp-Cl. Although these baffles have permeability which is an order of magnitude less than Type II rocks and presumably would yield lower flow rates, fines migration of kaolinite and illite may be problematic because pore throats are also smaller and could be more easily plugged. Certainly the illitic type III baffles are susceptible to fines migration (Wilson *et al*., 2014) whereas the more compacted depositional clay is less likely to migrate.

Type IV, V and VI barriers are mostly IV-Dp-Cl, with some IV-Dg-K and IV-Dg-Ifk,Ifb (Fig. 12). Some of these depositional barriers in the Basal Khuff Clastics and Unayzah A contain dolomitic zones that could be reactive with acidic fluids where they are interbedded with conduits and baffles.

Stratigraphic and environmental distribution of barriers, baffles and flow conduits

The storage and flow capacity of the different depositional facies can be visualized by plotting cumulative kh versus cumulative φh (Lorenz plot)

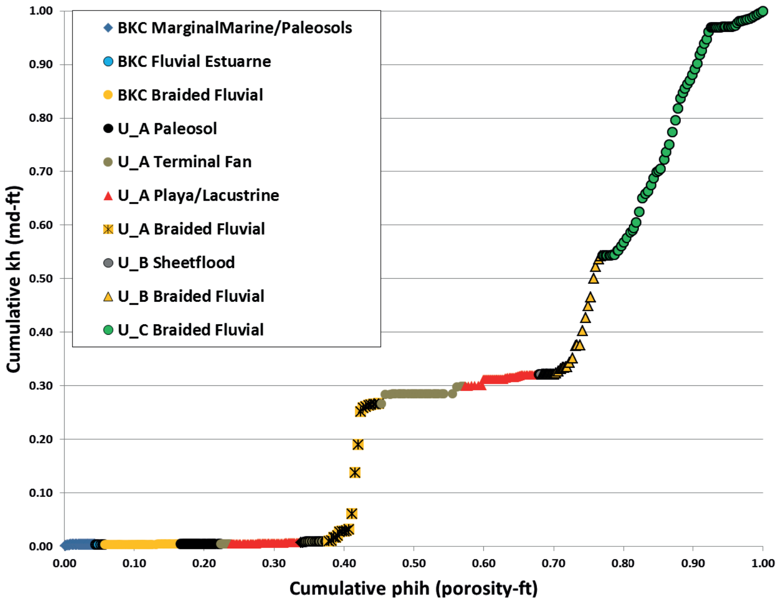

Fig. 13. Lorenz plot of well 1 showing depositional environments. Unayzah A, B and C braided fluvial sandstones provide the dominant fluid storage and flow capacity in this well.

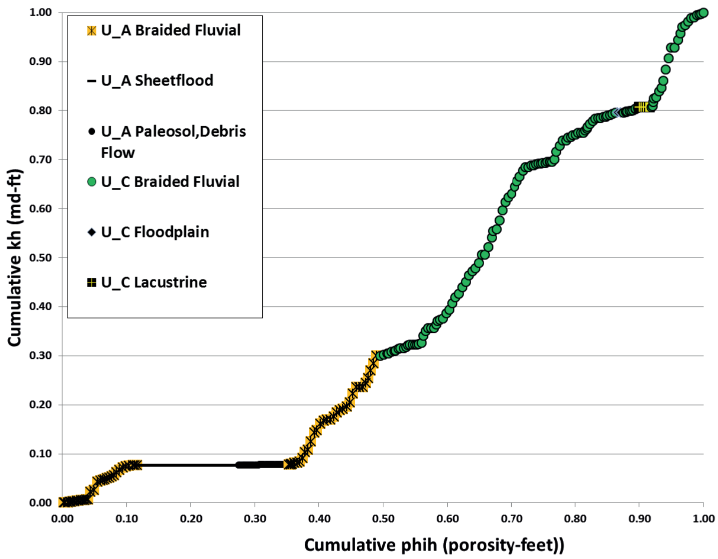

Fig. 14. Lorenz plot of well 2. Unayzah A and C braided stream sandstones provide excellent storage and flow capacity for fluids in this well.

(Figs 13-15). Well 1 exhibits a good section of kh through the Unayzah A braided stream section but does not add significant feet of porosity. Unayzah B and C braided stream deposits form a nearly continuous section of flow and storage capacity, accounting for about 32 % of the storage capacity of rocks in the well and about 68 % of the flow capacity (Fig. 13). Unayzah A playa and terminal fan deposits separate the Unayzah A flow conduits from those in the B and C. Breaks in slope in Fig. 13 can be used to further define and subdivide flow units within well 1 and the other wells (c.f. Gunter *et al*., 1997), but only the general trends are noted here.

In well 2, an upper section of Unayzah A braided stream deposits provides some flow and storage capacity and is separated from a second interval by Unayzah A sheetflood deposits and paleosols. The lower Unayzah A braided stream interval connects with the Unayzah C braided stream section which provides about 50% of the storage capacity and 70% of the flow capacity (Fig. 14).

Well 3 encountered a different set of depositional facies in the Unayzah A, mostly aeolian deposits. A thin interval of Basal Khuff Clastics fluvial-estuarine sandstones are porous and permeable, but they are separated from the Unayzah reservoir by paleosols and playa deposits in the upper part of the Unayzah A (Fig. 15). Essentially all the flow capacity and storage in the cored interval of this well is within aeolian dune sandstones. Dry interdune sandstone may be baffles or barriers, with wet interdune sandstones providing barriers within the aeolian dune interval.

The distribution of kh with stratigraphic unit and by environment is shown in Figs 16-18. In conjunction

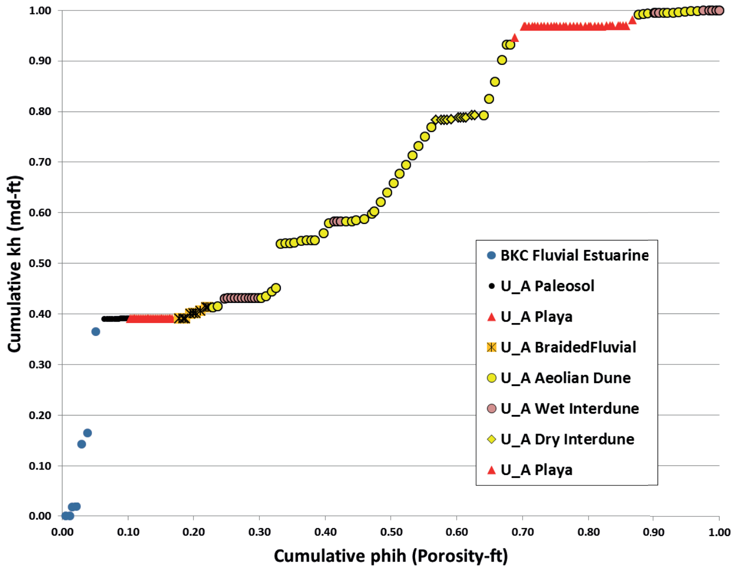

Fig. 15. Lorenz plot of well 3. A thin interval of BKC (Basal Khuff Clastics) fluvial estuarine sandstones exhibits some reservoir quality, but it is effectively separated from the Unayzah reservoir by paleosol and playa deposits in the upper Unayzah A. A thin interval of Unayzah A braided stream sandstones provides some storage and flow capacity, but most of the storage and flow capacity in this well is from Unayzah A aeolian dunes.

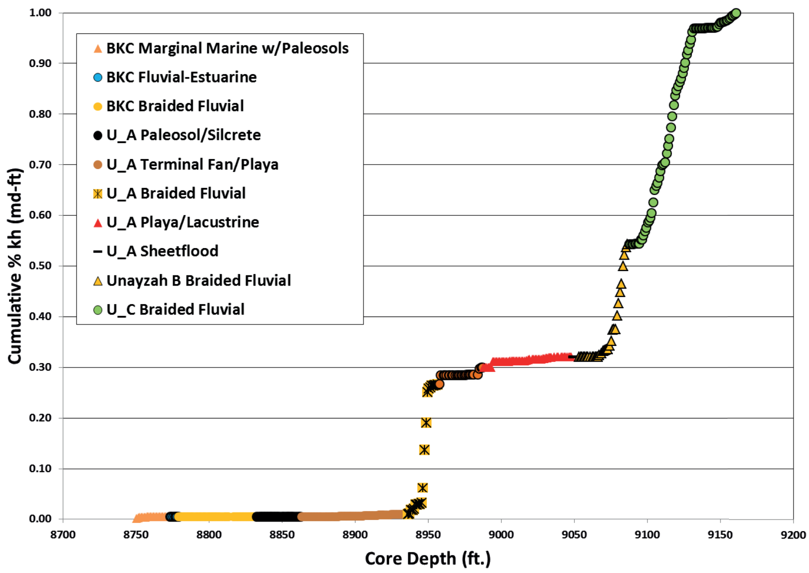

Fig. 16. Cumulative kH versus depth for well 1, showing depositional environments and stratigraphy.

with Figs 13-15 and the core descriptions in Fig. 19, it is possible to better visualize the large scale, stratigraphic controls on flow conduits, barrier and baffles. One of the more striking findings is that Basal Khuff Clastics braided stream sandstones are barriers to flow as opposed to the better flow and storage units in Unayzah A, B, and C braided stream deposits of roughly equivalent grain size. As discussed previously, this is a climatic effect. As with the clay cutans, the abundance of kaolinite in the Unayzah A and Basal Khuff Clastics may be due to periodic wetness during Unayzah A time and the overall more warm and humid climate during Basal Khuff Clastics time (Franks, 2008). The cutans are now mostly illitic (illite and low-expandibility I/S) (Polkowski, 1997), but originally were probably smectitic (Al-Ramadan, 2014).

It will be important to map the distribution of these flow barriers because they erode down into the Unayzah reservoir.

Likewise, it will be important to understand and map out the lateral relations of aeolian facies and braided stream facies of the Unayzah A. Although both facies contain significant thicknesses of porous and permeable sediment, the pore structure and nature of pore-filling phases is quite different.

CONCLUSIONS

Petrology and sedimentology have been combined with porosity and permeability data to evaluate the pore-level character of the Unayzah reservoir in Nuayyim field, central Saudi Arabia, and the effect

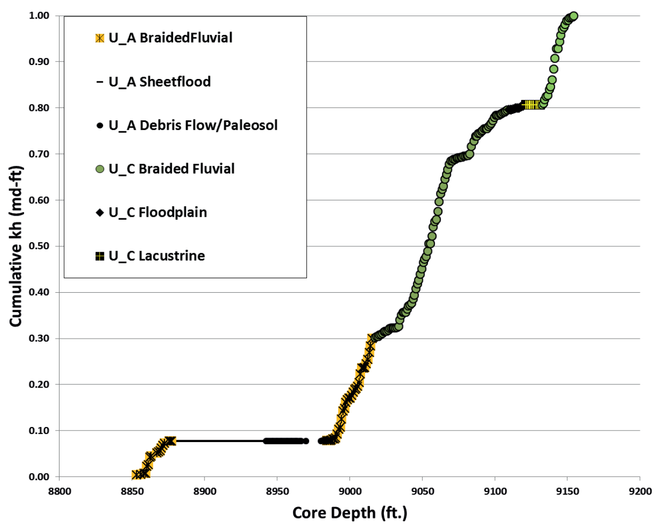

Fig. 17. Cumulative kH versus depth for well 2, showing depositional environments and stratigraphy.

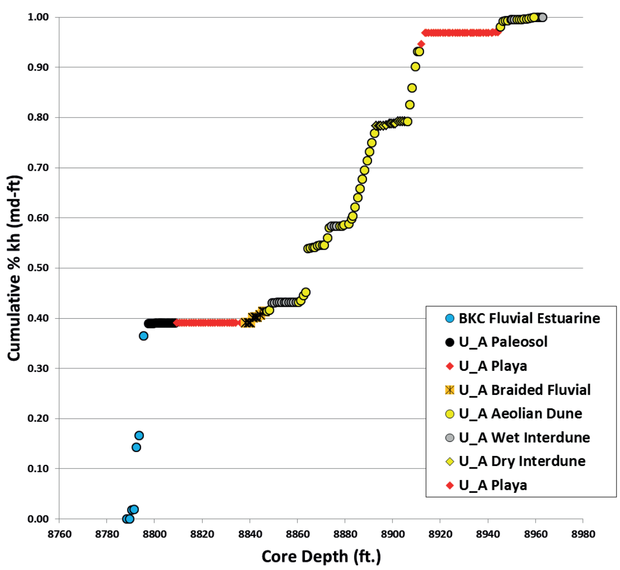

Fig. 18. Cumulative kH versus depth for well 3, showing depositional environments and stratigraphy.

these parameters have on flow and storage capacity. Barriers, baffles and flow conduits have been identified and described both in terms of pore-level character, depositional environment, and stratigraphic relations. Six rock types have been identified, one of which includes samples with microfractures of uncertain origin – perhaps artefacts of sampling. The other five define different types of flow conduits, barriers and baffles. The rock types have been further classified in terms of diagenetic versus depositional control on pore-level structure, and then additionally divided by the mineralogy of the pore-filling phase.

Braided steam deposits of the Basal Khuff Clastics are barriers to fluid flow. Pore spaces are filled mostly with depositional clay matrix and pseudomatrix of compacted rock fragments. Barriers within the Unayzah A are: (i) very fine sands and silts comprising playa/lacustrine deposits; (ii) fine and very fine wet interdune sands together with some very fine dry interdune sands; (iii) paleosols and debris flows; and (iv) silts and very fine to fine terminal fan and sheetflood sands. These barriers are plugged with diagenetic clay (illite, kaolinite) and in some cases with depositional and infiltrated clays. Baffles are primarily: (i) fine-medium sands within terminal fan and sheetflood deposits; (ii) thinner and finer aeolian dune sands; and (iii) coarser dry interdune sands. Diagenetic clay, particularly kaolinite and illite, partly plugs the pores. The best flow conduits and storage units are braided stream sandstones of the Unayzah A, B and C. These are medium to coarse sandstones, partly cemented with quartz overgrowths, with low amounts of diagenetic or depositional clay. Next best are the aeolian sand dunes of the Unayzah A with diagenetic kaolinite, chlorite, and illite.

The Unayzah reservoir is vertically compartmentalized within the Unayzah A, especially within the Unayzah A aeolian section. Flow conduits in the Unayzah B and C are in vertical communication (e.g. wells 1, 2) and in some cases flow conduits at the base of the Unayzah A are in vertical communication with flow conduits in the Unayzah B and C (e.g. well 2).

This study provides a starting point for evaluating the efficacy of future EOR projects and for the three-

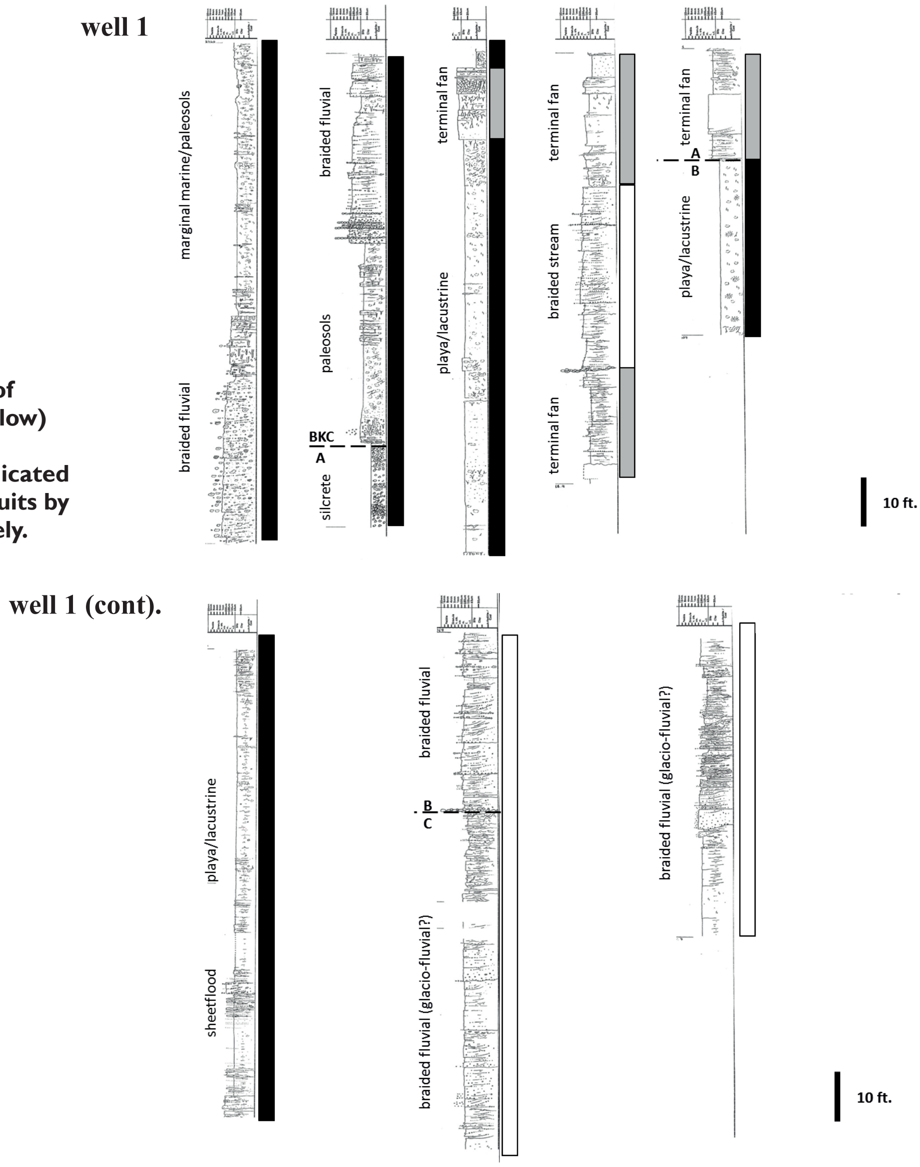

Fig. 19. (A) Core descriptions of well 1 (right, and continued below) with interpreted depositional environments. Barriers are indicated by black bars, baffles and conduits by grey and white bars, respectively.

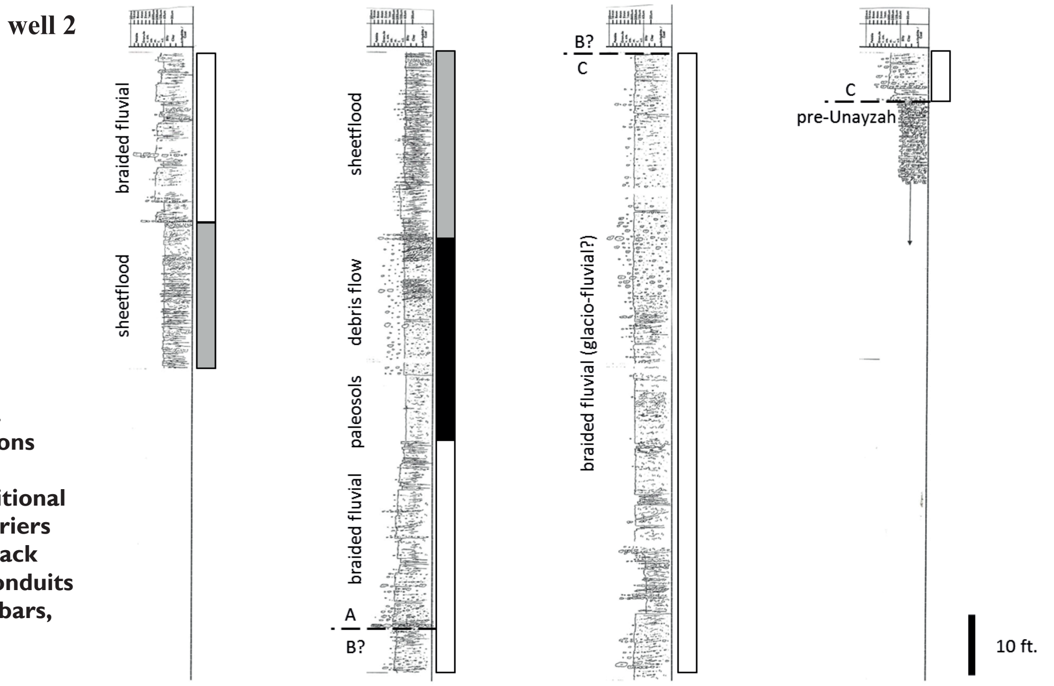

Fig. 19 (*continued*). (B) Core descriptions of well 2 with interpreted depositional environments. Barriers are indicated by black bars, baffles and conduits by grey and white bars, respectively.

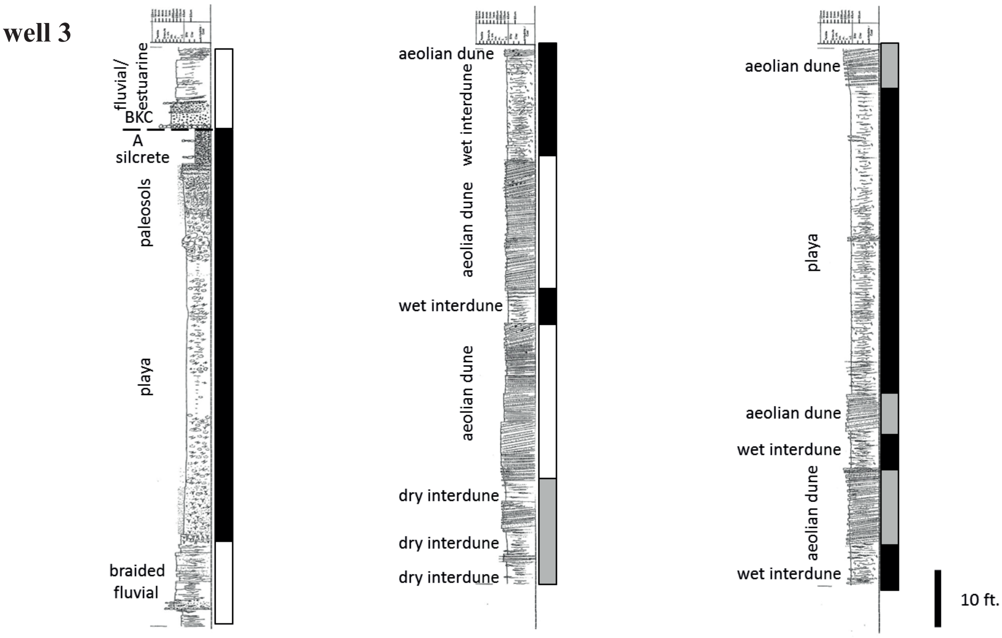

Fig. 19 (*continued*). (C) Core descriptions of well 3 with interpreted depositional environments. Barriers are indicated by black bars, baffles and conduits by grey and white bars, respectively.

dimensional mapping of flow conduits, barriers, and baffles using well logs, production data, and fluid geochemistry.

ACKNOWLEDGEMENTS

The authors would like to acknowledge support provided by King Abdul Aziz City for Science and Technology (KACST) through the National Science and Technology Initiative Program at King Fahd University of Petroleum and Minerals (KFUPM) (grant NSTIP # 09-OIL770-04). We would also like to thank Saudi Aramco for providing the core plugs and porosity/permeability data for the three wells and for permission to publish this study. We would like to thank Mr A. O. Amao for providing constructive suggestions to improve the images. John Pantano (Texas A&M University) provided valuable insight and discussions on the project and was a great sounding board for many of our ideas. We acknowledge with thanks journal review of a previous version by Martin Keller (University of Erlangen-Nuremberg) which improved the manuscript significantly.

REFERENCES

AKTAS, G. and COCKER, J.D. 1995. Diagenetic and depositional controls on reservoir quality in Khuff and Unayzah sandstones, Hawtah trend, central Saudi Arabia. In: Al-Husseini, M.I. (Ed.), Middle East Petroleum Geosciences Geo '94: Gulf Petrolink, Bahrain, **1**, 44–52.

AL-LABOUN, A. A., 1987. Unayzah Formation: A new Permo-Carboniferous Unit in Saudi Arabia. *AAPG Bull.,* **71**, 29–38.

AL-RAMADAN, K., 2014. Illitization of Smectite in Sandstones: The Permian Unayzah Reservoir, Saudi Arabia. *Arabian Journal for Science and Engineering*, **39**, 407-412.

ARCHIE, G.E., 1950. Introduction to petrophysics of reservoir rocks. *AAPG Bull.*, **34**, 943-961.

DOTT, R. H., JR., 1964. Wacke, graywacke and matrix-- what approach to immature sandstone classification?. *Journal of Sedimentary Petrology*, **34**, 625-632.

EBANKS, W.J., Jr., M.H. SCHEIHING and C. D. ATKINSON, 1992. Flow units for reservoir characterization. In: D. Morton-Thompson, A.M. Woods (Eds), Development Geology Reference Manual. *AAPG Methods in Exploration Series* **10**, 282-284.

FRANKS, 2008. From plate to pore: plate motion, paleoclimate, paleosols, and porosity in the Permo-Carboniferous Unayzah reservoir sandstones of Saudi Arabia. AAPG International Conference Poster Session, Capetown, South Africa, October, *AAPG Search and Discovery Article* #51117.

FRANKS, S.G. and H. ZWINGMANN, 2010. Origin and timing of late diagenetic illite in the Permian-Carboniferous Unayzah sandstone reservoirs of Saudi Arabia. *AAPG Bull.* **94**, 1133–1159.

GRAY, D.H. and R.W. REX, 1966. Formation damage in sandstones caused by clay dispersion and migration. *Clays and Clay Minerals*, **15**, 355-366.

GUNTER, G.W., J.M. FINNERAN, D.J. HARTMANN and J.D. MILLER, 1997. Early determination of reservoir flow units using an integrated petrophysical method. 1997 SPE Annual Tech, Conf. and Exhib., *SPE Paper* 38679, 8pp.

HURST, A. and P.H. NADEAU, 1995. Clay microporosity in reservoir sandstones: an application of quantitative electron microscopy in petrophysical evaluation. *AAPG Bull.*, **79,** 4, 563-573.

KOLODZIE, S., Jr., 1980. Analysis of pore throat size and use of the Waxman-Smits equation to determine OOIP in Spindle Field, Colorado. Society of Petroleum Engineers, 55th Annual Fall Technical Conference, Paper SPE-9382, 10 pp.

KONERT, G., A.M. AFIFI, S.A. AL-HAJRI and H.J. DROSTE, 2001. Paleozoic stratigraphy and hydrocarbon habitat of the Arabian Plate. *GeoArabia,* **6**, 3, 407–442.

McGILLIVRAY, J.G., and AL-HUSSEINI, M.I. 1992. The Paleozoic petroleum geology of central Arabia. *AAPG Bull.* **76**, 10, 1473–1490.

MELVIN, J. and R.A. SPRAGUE, 2006. Advances in Arabian stratigraphy: Origin and stratigraphic architecture of glaciogenic sediments in Permian-Carboniferous lower

Unayzah sandstones, eastern central Saudi Arabia. *GeoArabia*, **11**, 105–152.

MELVIN, J., R.A. SPRAGUE and C. J. HEINE, 2010. From bergs to ergs: The late Paleozoic Gondwanan glaciation and its aftermath in Saudi Arabia. In: O.R. Lopez-Gamundi and L.A. Buatois (Eds), Late Paleozoic Glacial Events and Postglacial Trangressions in Gondwana. *Geological Society of America Special Paper* **468,** 37-80.

PITTMAN, E.D., 1992. Relationship of porosity and permeability to various parameters derived from mercury injection-capillary pressure curves for sandstone. *AAPG Bull.,* **76,** 191–198.

PITTMAN, E.D., 2001. Estimating pore throat size in sandstones from routine core-analysis data. *Search and Discovery Article* #40009, 20 pp.

POLKOWSKI, G.R., 1997. Degradation of reservoir quality by clay content, Unayzah Formation, Central Saudi Arabia. *GeoArabia,* **2,** 49–64.

SARDINI, P., A. EL ALBANI, S. GABOREAU, M. SIITARI-KAUPPI, and D. BEAUFORT, 2009. Mapping and quantifying the clay aggregate microporosity in medium- to coarse-grained sandstones using the 14C-PMMA method. *Journal of Sedimentary Research,* **79**, 584-592.

SENALP, M. and A. AL-DUAIJI, 2001. Stratigraphy and sedimentation of the Unayzah Reservoir, central Saudi Arabia. In: M.I. Husseini (Ed.), Geo '94, The Middle East Petroleum Geosciences, Gulf Petrolink, Bahrain, p. 837–847.

WILSON, M.J., L. WILSON, and I. PATEY, 2014. The influence of individual clay minerals on formation damage of reservoir sandstones: a critical review with some new insights. *Clay Minerals*, **49,** 147-164.